Biotribology xxx (xxxx) xxx–xxx

Contents lists available at ScienceDirect

Biotribology

journal homepage: www.elsevier.com/locate/biotri

Spherically capped membrane probes for low contact pressure tribology

Samantha L. Marshall[a], Kyle D. Schulze[a], Samuel M. Hart[a], Juan Manuel Urueña[a], Eric O. McGhee[a], Alexander I. Bennett[a], Angela A. Pitenis[a], Christopher S. O'Bryan[a], Thomas E. Angelini[a], W. Gregory Sawyer[a,b,*]

[a] Department of Mechanical and Aerospace Engineering, University of Florida, Gainesville, FL 32611, United States
[b] Department of Materials Science and Engineering, University of Florida, Gainesville, FL 32611, United States

ARTICLE INFO

Keywords:
Hydrogel
Indentation
Contact mechanics
In situ tribology
Microtribology

ABSTRACT

Low contact pressure measurements are needed for biotribology studies on cells, cell layers, and tissues. Such studies typically require low forces to achieve kPa range contact pressures, but such methods frequently come at the expense of contact area and, in turn, relevance. In seeking lower contact pressures, the corresponding contact areas can become too small to be physiologically relevant or important. The recently developed method creates probes that are thin spherical shells, specifically designed to create low contact pressures. These polyethylene glycol and polyacrylamide hydrogel probes were polymerized with embedded fluorescent nanoparticles, and indentation experiments were performed *in situ* on a confocal microscope to determine the deformation mechanics. The indentation load *versus* contact width behavior revealed that this design has the ability to achieve pressures in the kPa range at macroscopic contact areas that are independent of the applied load (*i.e.*, the area grows linearly with the applied load, leading to a constant contact pressure).

1. Introduction

The cornea is made up of moist epithelial cells that form a thin stratified layer on the exterior surface of the eye. This layer is protected by a mucinated aqueous tear film, and both vision and ocular health are dependent upon the stability of the tear film [1]. This protective aqueous film is dynamically maintained by the corneal and conjunctival epithelia [2,3]. Under conditions of contact lens use, disruption of the tear film can lead to discomfort and cell damage [4]. Contact lens design and material selection balances contact pressure and lubricity in an effort to maintain comfort and function over a wide range of sliding conditions during ocular movements while minimizing damage to the epithelia [5–7]. The contact pressures exerted on the cornea by the eyelid are estimated to be 1–5 kPa [8] and may increase to 12–18 kPa [9] with the inclusion of a soft hydrogel-based contact lens. Matching the contact pressure conditions is essential for *in vivo* [9–11], *ex vivo*, [12] and *in vitro* [10,13–18] studies that aim to collect physiologically relevant friction measurements.

In vitro biotribological experiments using a spherical probe sliding against a cellular monolayer [13–15] are desirable for *in situ* studies. However, even the softest hydrogel materials have been observed to severely damage the cellular monolayer during sliding due to high contact pressures that result from the Hertzian mechanics of a solid spherical probe. As an example, a hydrogel probe with an elastic modulus on the order of 20 kPa and a diameter of a few millimeters can routinely produce contact pressures in excess of 10 kPa at normal loads below 500 μN [19]. Even for sophisticated microtribometers, such studies prove to be extremely challenging. For cells grown in culture, setup of *in situ* experiments often involves metrology that is not optimal for high-precision tribological experiments, and small misalignments in setup over long sliding distances can cause large variations in contact pressure. These studies are often laborious, tedious, and frequently lead to unacceptable variations in contact conditions along the track, thereby frustrating analysis and limiting applicability.

We have developed a probe geometry that uses a spherically capped shell or membrane, as shown schematically in Fig. 1. This geometry capitalizes on the mechanics of the geometry such that, at low forces (μN) and strains, the contact pressure is predicted and found to be constant and independent of the applied load. Such a probe allows the contact area to fluctuate with variations in applied load without changing the average contact pressure, making the design extremely attractive and practical for low pressure measurements in biotribology.

* Corresponding author at: Department of Mechanical and Aerospace Engineering, University of Florida, Gainesville, FL 32611, United States.
E-mail address: wgsawyer@ufl.edu (W.G. Sawyer).

http://dx.doi.org/10.1016/j.biotri.2017.03.008
Received 14 November 2016; Received in revised form 1 March 2017; Accepted 6 March 2017

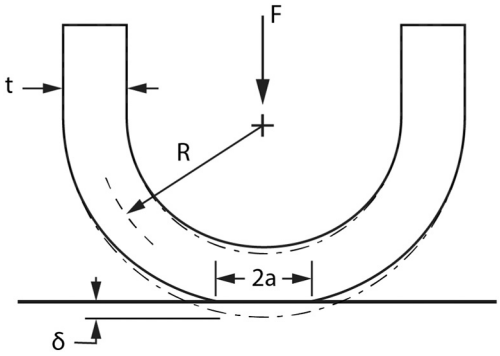

Fig. 1. Schematic of the spherical shell probe with thickness t and radius R. The probe is pressed against a glass-bottom culture dish with a normal force F, and with the resulting contact width $2a$. The deflection of the probe tip is given by δ.

2. Materials and methods

2.1. Material preparation

The spherical shell hydrogel probes (2 mm radius of curvature and thickness of 1.5 mm) were fabricated using two different methods: (1) casting in a mold, and (2) three-dimensional (3D) printing in a soft granular microgel media liquid-like solid (LLS). The molding approach used standard polymerization protocols that can be found in the literature [20] with a 1 mm smooth nylon rod inserted into the center of the mold. The probes were made from 7.5% (w/w) polyacrylamide and were doped with 25 nm green fluorescent beads prior to polymerization. The embedded fluorescent beads allowed the probes to be imaged by a confocal microscope when submerged in water. Solute constituents and weight percentages were consistent with those used by Urueña et al. [20] and produced a hydrogel with a modulus of approximately 20 kPa. The rod and probe were then removed from the mold and the molded probe was fitted to a nylon fastener.

Hydrogel probes were also 3D-fabricated using the LLS soft granular microgels as described in Bhattacharjee et al. [21–23], using a polyethylene glycol (PEG) hydrogel. These PEG hydrogels were prepared at a ~11 wt% poly(ethylene glycol) acrylate monomethyl ether and ~2.5 wt% poly(ethylene glycol) diacrylate concentration in ultrapure water (18.2 MΩ); less than 0.05 wt% Irgacure D-2959 was added as an ultraviolet (UV) photoinitiator. The probe was printed in a microgel medium made of 0.1% ETD2020 carbomer suspended in ultrapure water [21–23]. A steel needle with a 190 μm inner diameter was used for printing, and the resulting printed probes were cured for 5 min under UV illumination. The probe was removed from LLS media, swelled to equilibrium in ultrapure water for 24 h.

2.2. Experimental methods

Indentations were performed on a custom microindenter described in Schulze et al. attached to a Nikon C2 Eclipse Ti confocal laser-scanning microscope [24]. The apex of the probe was aligned with the optical axis of the microscope objective. Prior to indentation, a z-stack of images (1300 μm × 1300 μm × approximately 2 mm) was taken on the confocal fluorescence microscope to measure the un-deformed probe shape (Fig. 2a). The hydrogel probe was then loaded against a glass-bottom culture dish coated with Pluronic® F-127 to minimize adhesion effects under submerged conditions (Fig. 2b). All indentation experiments were performed with the probe fully submerged in ultrapure water. The applied load was monotonically increased from 50 μN to 1000 μN through load-controlled, closed-loop feedback control. At each discrete indentation load, confocal imaging with fluorescein isothiocyanate filtering was used to reconstruct a 3D representation of the deformation and contact area using the embedded fluorescent green particles (see Fig. 2b).

3. Results

The radius of curvature of the probe R was measured using a z-stack image at zero load. To measure contact the z-stacks taken at every indentation load F_n were rotated and a slice was taken in the plane perpendicular to the surface. To measure the contact at each load, X-Z slices from the 3D intensity distribution were analyzed, effectively viewing the deformed probe from the side. To enhance the differences between contacting and noncontacting regions, these X-Z images were stretched by a factor of 2.5 in the Z-direction. The contact width $2a$ is apparent in these images and was measured manually using ImageJ software. The development of the contact radius as a function of the indentation force is shown in Fig. 2c. The indentation revealed a constant pressure in which the contact width increases with load to a 1/2 power up to a contact radius of approximately 300 μm, at which point the behavior changes and the contact width increases more slowly with increases in load.

4. Discussion

The low contact pressure achievable through this design was expected, but the constant pressure with applied load was initially a surprise. Following Roark's analysis of a simply supported circular plate along the edge with a point load [25] gives the maximum deflection δ as shown by Eq. (1): where F is the force, R is the radius of curvature, E is the elastic modulus, t is the thickness of the spherical shell, and ν is the Poisson ratio.

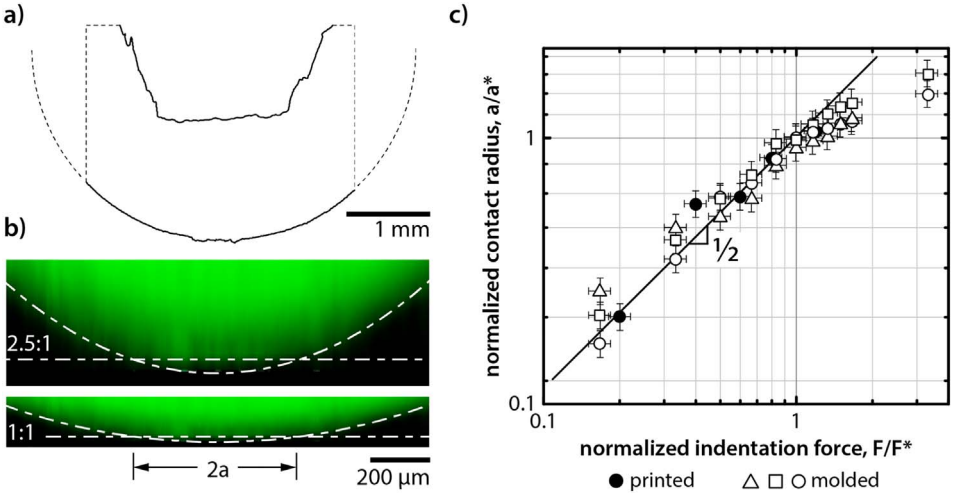

Fig. 2. (a) Line profile of a molded spherical shell probe from a confocal 3D reconstruction. (b) Confocal imaging of a probe (E ~ 20 kPa) indenting a glass surface under 250 μN of load. The contact region is shown. The hydrogel contains fluorescent beads to allow imaging. (c) Log-log plot of normalized indentation force F/F^* *versus* the normalized contact radius a/a^*. Before a critical point, the probe acts as a gentle, constant pressure interface dictated by its elastic modulus. Exceeding this normal force, the spherical shell probe no longer acts as a constant pressure system.

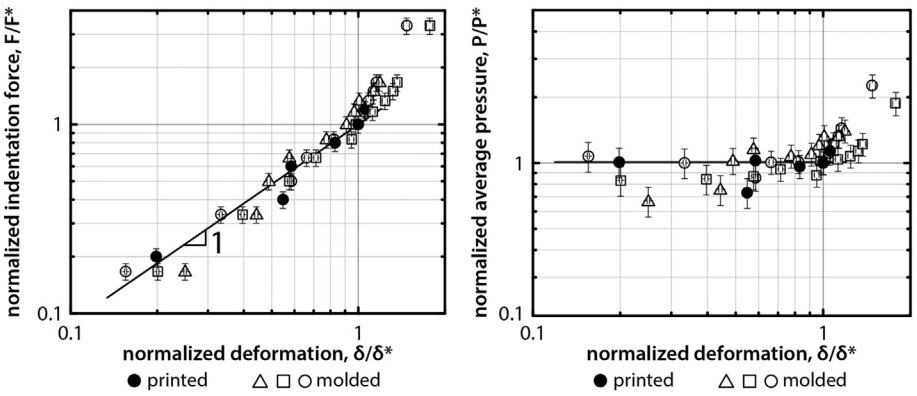

Fig. 3. (a) Deformation *versus* indentation force data showing a direct power relationship between deformation and indentation force in the low force regime. (b) Deformation *versus* average pressure data. In the low force regime, the average pressure is independent of the deformation.

$$\delta = \frac{FR^2}{4\pi Et^2}\cdot 3(1-\nu^2) \tag{1}$$

Through a combination of terms and using the small-angle approximation ($a = \sqrt{2R\delta}$), the pressure P of a centrally loaded region of a circular plate can be shown to be proportional to the product of the modulus E and the geometry terms cubed as shown in Eq. (2), independent of the applied load.

$$P \propto E\left(\frac{t}{R}\right)^3 \tag{2}$$

Similarly, the equations for the deflection and pressure on the apex of a spherical shell with a concentrated load on a small circular area at the pole reveal that the pressure P is again proportional to the product of the modulus E and the geometry terms squared as shown in Eqs. (3) and (4).

$$\delta \propto \frac{FR}{Et^2} \tag{3}$$

$$P \propto E\left(\frac{t}{R}\right)^2 \tag{4}$$

For both estimations the pressure is independent of the contact area and relies only on material properties and geometry.

The mechanics of the spherically capped probe have been successfully utilized to directly apply single kPa contact pressures on a monolayer of corneal epithelial cells over the course of nearly 24 h without causing any cell death [26].

5. Conclusion

We have demonstrated that the production of spherically capped shells provides a convenient method to perform low contact pressure experiments. Under low deformations, these probes give constant contact pressure independent of the applied load or contact deflection (Fig. 3). This is in comparison to full hemispherical probes that follow Hertzian contact [27,28]. Both the molded and the 3D-printed probes experience a constant contact pressure up to approximately 300 μN and 250 μN, respectively. Using a similar technique an experimentalist could not only apply low, direct, and previously inaccessible contact pressures, but also alleviate force variation due to alignment. For cell monolayers where a change in force or pressure can cause cell rupture, these considerations become extremely critical.

Acknowledgements

This work was funded by Alcon Laboratories.

References

[1] J. Murube, Etymology of the term “tear”, Ocul. Surf. 3 (2005) 177–181, http://dx.doi.org/10.1016/S1542-0124(12)70203-3.

[2] R.J. Braun, P.E. King-Smith, C.G. Begley, L. Li, N.R. Gewecke, Dynamics and function of the tear film in relation to the blink cycle, Prog. Retin. Eye Res. 45 (2015) 132–164, http://dx.doi.org/10.1016/j.preteyeres.2014.11.001.

[3] J.M. Coles, D.P. Chang, S. Zauscher, Molecular mechanisms of aqueous boundary lubrication by mucinous glycoproteins, Curr. Opin. Colloid Interface Sci. 15 (2010) 406–416, http://dx.doi.org/10.1016/j.cocis.2010.07.002.

[4] P.J. Murphy, S. Patel, J. Marshall, The effect of long-term, daily contact lens wear on corneal sensitivity, Cornea 20 (2001) 264–269, http://dx.doi.org/10.1097/00003226-200104000-00006.

[5] A.C. Dunn, J.A. Tichy, J.M. Urueña, W.G. Sawyer, Lubrication regimes in contact lens wear during a blink, Tribol. Int. 63 (2013) 45–50, http://dx.doi.org/10.1016/j.triboint.2013.01.008.

[6] M. Roba, E.G. Duncan, G.A. Hill, N.D. Spencer, S.G.P. Tosatti, Friction measurements on contact lenses in their operating environment, Tribol. Lett. 44 (2011) 387–397, http://dx.doi.org/10.1007/s11249-011-9856-9.

[7] S. de Beer, M.H. Müser, Alternative dissipation mechanisms and the effect of the solvent in friction between polymer brushes on rough surfaces, Soft Matter 9 (2013) 7234, http://dx.doi.org/10.1039/c3sm50491c.

[8] H.D. Conway, M.W. Richman, The effects of contact lens deformation on tear film pressure and yhickness during motion of the lens towards the eye, J. Biomech. Eng. 105 (1983) 47, http://dx.doi.org/10.1115/1.3138383.

[9] A.C. Dunn, J.M. Urueña, E. Puig, V.L. Perez, W.G. Sawyer, Friction coefficient measurement of an in vivo murine cornea, Tribol. Lett. 49 (2013) 145–149, http://dx.doi.org/10.1007/s11249-012-0033-6.

[10] T.E. Angelini, A.C. Dunn, J.M. Urueña, D.J. Dickrell, D.L. Burris, W.G. Sawyer, Cell friction, Faraday Discuss. 156 (2012) 31, http://dx.doi.org/10.1039/c2fd00130f.

[11] R.C. Barros, T.G. Van Kooten, D.H. Veeregowda, Investigation of friction-induced damage to the pig cornea, Ocul. Surf. 13 (2015) 315–320, http://dx.doi.org/10.1016/j.jtos.2015.05.004.

[12] T. Wilson, R. Aeschlimann, S. Tosatti, Y. Toubouti, J. Kakkassery, K. Osborn Lorenz, Coefficient of friction of human corneal tissue, Cornea 34 (2015) 1179–1185, http://dx.doi.org/10.1097/ICO.0000000000000524.

[13] J.A. Cobb, A.C. Dunn, J. Kwon, M. Sarntinoranont, W.G. Sawyer, R. Tran-Son-Tay, A novel method for low load friction testing on living cells, Biotechnol. Lett. 30 (2008) 801–806, http://dx.doi.org/10.1007/s10529-007-9623-z.

[14] J.P. Straehla, F.T. Limpoco, N.V. Dolgova, B.G. Keselowsky, W.G. Sawyer, S.S. Perry, Nanomechanical probes of single corneal epithelial cells: shear stress and elastic modulus, Tribol. Lett. 38 (2010) 107–113, http://dx.doi.org/10.1007/s11249-010-9579-3.

[15] A.C. Dunn, T.D. Zaveri, B.G. Keselowsky, W.G. Sawyer, Macroscopic friction coefficient measurements on living endothelial cells, Tribol. Lett. 27 (2007) 233–238, http://dx.doi.org/10.1007/s11249-007-9230-0.

[16] A.C. Dunn, J.A. Cobb, A.N. Kantzios, S.J. Lee, M. Sarntinoranont, R. Tran-Son-Tay, W.G. Sawyer, Friction coefficient measurement of hydrogel materials on living epithelial cells, Tribol. Lett. 30 (2008) 13–19, http://dx.doi.org/10.1007/s11249-008-9306-5.

[17] G. Hofmann, P. Jubin, P. Gerligand, A. Gallois-Bernos, S. Franklin, N. Smulders, L.C. Gerhardt, S. Valster, In-vitro method for determining corneal tissue friction and damage due to contact lens sliding, Biotribology 5 (2016) 23–30, http://dx.doi.org/10.1016/j.biotri.2016.01.001.

[18] E.D. Bonnevie, V.J. Baro, L. Wang, D.L. Burris, Fluid load support during localized indentation of cartilage with a spherical probe, J. Biomech. 45 (2012) 1036–1041, http://dx.doi.org/10.1016/j.jbiomech.2011.12.019.

[19] E. Van Der Heide, X. Zeng, M.A. Masen, Skin tribology: science friction? Friction 1 (2013) 130–142, http://dx.doi.org/10.1007/s40544-013-0015-1.

[20] J.M. Urueña, A.A. Pitenis, R.M. Nixon, K.D. Schulze, T.E. Angelini, W. Gregory Sawyer, Mesh size control of polymer fluctuation lubrication in gemini hydrogels, Biotribology 1–2 (2015) 24–29, http://dx.doi.org/10.1016/j.biotri.2015.03.001.

[21] T. Bhattacharjee, S.M. Zehnder, K.G. Rowe, S. Jain, R.M. Nixon, W.G. Sawyer, T.E. Angelini, Writing in the granular gel medium, Sci. Adv. 1 (2015) e1500655, http://dx.doi.org/10.1126/sciadv.1500655.

[22] T. Bhattacharjee, C.J. Gil, S.L. Marshall, J.M. Urueña, C.S. O'Bryan, M. Carstens, B. Keselowsky, G.D. Palmer, S. Ghivizzani, C.P. Gibbs, W.G. Sawyer, T.E. Angelini, A.C.S.B. Science, Liquid-like solids support cells in 3D, ACS Biomater. Sci. Eng. (2016) (acsbiomaterials.6b00218), http://dx.doi.org/10.1021/acsbiomaterials.6b00218.

[23] K.J. LeBlanc, S.R. Niemi, A.I. Bennett, K.L. Harris, K.D. Schulze, W.G. Sawyer, C. Taylor, T.E. Angelini, Stability of high speed 3D printing in liquid-like solids, ACS Biomater. Sci. Eng. (2016) (acsbiomaterials.6b00184), http://dx.doi.org/10.1021/acsbiomaterials.6b00184.
[24] K.D. Schulze, S.M. Zehnder, J.M. Urueña, W.G. Sawyer, T.E. Angelini, Elastic modulus and hydraulic permeability of MDCK monolayers, J. Biomech. (2017) 2–5, http://dx.doi.org/10.1016/j.jbiomech.2017.01.016.
[25] W.C. Young, R.G. Budynas, Roark's Formulas for Stress and Strain, (2002), http://dx.doi.org/10.1002/9780470974414.part3.
[26] A.A. Pitenis, J.M. Urueña, T.T. Hormel, T. Bhattacharjee, S.R. Niemi, S.L. Marshall, S.M. Hart, K.D. Schulze, T.E. Angelini, W.G. Sawyer, Corneal cell friction: Survival, lubricity, tear films, and mucin production over extended duration in vitro studies, Biotribology (2017), http://dx.doi.org/10.1016/j.biotri.2017.04.003.
[27] K.D. Schulze, A.I. Bennett, S.L. Marshall, K.G. Rowe, A.C. Dunn, Real area of contact in a soft transparent interface by particle exclusion microscopy, ASME J. Tribol. (2016) 1–6, http://dx.doi.org/10.1115/1.4032822.
[28] P.C. Nalam, N.N. Gosvami, M.A. Caporizzo, R.J. Composto, R.W. Carpick, Nano-rheology of hydrogels using direct drive force modulation atomic force microscopy, Soft Matter 11 (2015) 1–3, http://dx.doi.org/10.1039/C5SM01143D.